

## Structural Changes to Aspen Wood Lignin during Autohydrolysis Pretreatment

Peng Wang,<sup>a</sup> Yingjuan Fu,<sup>a,\*</sup> Zhiyong Shao,<sup>a</sup> Fengshan Zhang,<sup>b</sup> and Menghua Qin<sup>a,b,c,\*</sup>

Aspen wood was subjected to autohydrolysis as a pre-treatment to characterize the structural changes occurring in lignin fractions during the pre-treatment process. Milled wood lignin (MWL) was isolated from both the native aspen wood and hydrolyzed wood chips, and its structural features were characterized by Fourier transform infrared (FT-IR), quantitative <sup>13</sup>C, two-dimensional heteronuclear single quantum coherence (2D HSQC), and <sup>31</sup>P nuclear magnetic resonance (NMR) spectroscopies, gel permeation chromatography/multi-angle laser light scattering (GPC-MALLS), and thermal analysis. The lignin remaining in the hydrolyzed wood chips revealed more phenolic OH groups, fewer aliphatic OH groups, higher syringyl/guaiacyl ratios (S/G), higher molecular weights, and narrower polydispersities than the native lignin of aspen wood. The inter-unit linkages of  $\beta$ -O-4 were noticeably cleaved, but the condensed structures in the lignin formed when undergoing autohydrolysis of high severity, resulting in elevated amounts of C-C linkages. Moreover, it was found that autohydrolysis promoted the removal of -OCH<sub>3</sub> groups and increased the thermal stability of lignin fractions.

*Keywords:* Aspen; Autohydrolysis; Lignin; Structure change; Repolymerization of lignin

*Contact information:* a: Key Laboratory of Pulp & Paper Science and Technology of the Ministry of Education, Qilu University of Technology, Jinan 250353, Shandong, China; b: Huatai Group Corp. Ltd., Dongying, Shandong, 257335, China; c: Organic Chemistry Laboratory, Taishan University, Taian 271021, Shandong, China; \*Corresponding authors: fyingjuan@163.com; qmh@qlu.edu.cn

### INTRODUCTION

Lignocellulosic biomass, which primarily consists of lignin, cellulose, and hemicellulose, is the most abundant renewable resource on the earth and has great potential to be the basic organic source for green chemicals, energy, and materials (Amidon and Liu 2009; Ligeró *et al.* 2011). Based on the efficient and comprehensive utilization of each fraction of the biomass at the highest value, the biorefinery concept has been put forward (Ruiz *et al.* 2013). In particular, the concept of an integrated forest biorefinery (IFBR), in which fuels as well as higher value-added bio-based chemicals and materials are produced in addition to the traditional pulps, has been considered as the most practicable one (van Heiningen 2006; Zhu and Pan 2010; Xiao *et al.* 2013). However, being comparatively recalcitrant in nature (Zakaria *et al.* 2015), the lignocellulosic biomass must be subjected to successive processing stages to fractionate the main macromolecular components. Therefore, the pre-extraction of the raw materials prior to pulping is a significant step (Hou *et al.* 2014). Subsequently, each fraction is further processed to marketable products. From the pre-extracted liquid fraction, it is possible to obtain xylo-oligosaccharides, to extract phenolic antioxidants, and to produce ethanol by fermentation and xylitol by bioconversion, while the solid fraction can be used for the production of pulp or some value-added

products.

Some commonly used processes for pre-extraction of lignocellulosic materials are dilute acid hydrolysis, alkali treatment, and hydrothermal treatments such as steam-explosion, wet oxidation, microwave treatment, and autohydrolysis (Carvalho *et al.* 2009; Zhu and Pan 2010; Ruiz *et al.* 2013; Guo *et al.* 2015). Among these, autohydrolysis has the advantage of a high recovery of hemicelluloses as soluble saccharides, while both cellulose and lignin can be recovered in the solid phase with minor losses (Carvalho *et al.* 2009; Liu 2010; Ligeró *et al.* 2011). During the autohydrolysis process, acetic acid is released by hydrolysis of the acetyl groups in hemicelluloses (El Hage *et al.* 2010; Ligeró *et al.* 2011; Zhu *et al.* 2015), thus increasing the hydronium concentration in the reaction media (Zhu *et al.* 2015) and enabling the hydrolysis and the dissolution of a great part of the hemicelluloses and the cleavage of lignin-carbohydrate bonds (El Hage *et al.* 2010). Meanwhile, part of the lignin undergoes structural modifications and/or is depolymerized into small molecular fragments, resulting in the dissolution of small quantities of lignin (Leschinsky *et al.* 2008a). However, lignin repolymerization reactions have been found to take place simultaneously with lignin depolymerization during the autohydrolysis process (Li and Gellerstedt 2008). Particularly, pretreating the lignocellulosic materials at high severity will promote condensation reactions in lignin, inhibiting the downstream processing. On the other hand, a certain amount of colloiddally dissolved lignin or lignin-rich compounds will arise and generate uncontrollable precipitation after cooling, resulting in serious problems for further processing (Leschinsky *et al.* 2008a; Gütsch *et al.* 2012).

The characteristics of lignin influence the substrate saccharification, high-value utilization of lignin (Zhu and Pan 2010), and the pulping process of the solid fractions (Wen *et al.* 2013b). The properties of lignin differ with its source and the methods used to extract it (Zamudio *et al.* 2015). It is well known that the lignin content and its composition in terms of *p*-hydroxyphenyl (H), guaiacyl (G), and syringyl (S) moieties, as well as the nature of the different inter-unit linkages present in its structure, are important factors in pulp production, affecting the delignification rates, chemical consumption, and pulp yields (Rencoret *et al.* 2009). The initial hydrothermal pretreatment was found to be conducive to the subsequent alkaline fractionation of lignocellulosic materials (Sun *et al.* 2015). Rauhala *et al.* (2011) reported that autohydrolysis of birch wood caused a significant increase in the delignification rate during subsequent alkaline cooking processes. García *et al.* (2011) also found that autohydrolyzed chips required 16.6% less alkali than regular chips to achieve a kappa number of 33 for soda-anthraquinone pulping, and the obtained pulp had a good yield and viscosity. The reason for the enhanced delignification after autohydrolysis has been suggested to be associated with the cleavage of aryl-ether bonds, resulting in lignin depolymerization and the formation of new phenolic hydroxyl groups (Leschinsky *et al.* 2008b). However, when autohydrolysis severity is high, the overall delignification rate during kraft pulping decreases (Leschinsky *et al.* 2008a,b). The explanation proposed for this decrease is the difficulty in removal of lignin after intense thermal treatments because of lignin repolymerization through formation of a carbonium ion intermediate, which promotes the formation of new linkages of  $\beta$ - $\beta$ ,  $\beta$ -5, and  $\beta$ -1 types (Li *et al.* 2000). According to Fasching *et al.* (2005), autohydrolysis can lead to deactivation of the lignin for subsequent sulfonation reactions. The decrease in aliphatic OH groups, which represent the reaction sites in lignin for sulfonation, is primarily responsible for the deactivation of the lignin (Leschinsky *et al.* 2008b) itself. Therefore, the structural features and the fundamental chemistry of the lignin during the pretreatment process should be thoroughly

investigated (Wen *et al.* 2013c), which is of considerable importance in the ensuing delignification and bleaching steps (Jääskeläinen *et al.* 2003).

Aspen, one of the fastest growing wood species, is an attractive feedstock for use in the biorefinery framework. Much work has been devoted to understanding the effects of autohydrolysis pretreatment on characteristics of the autohydrolysis liquor and hydrolyzed chips (Hou *et al.* 2014). Moreover, many studies have been carried out on the kinetics and mechanism of autohydrolysis (Li and Gellerstedt 2008; Chen *et al.* 2010), which can separate lignin into two fractions: dissolved lignin in the autohydrolysis liquor and insoluble lignin remaining in the residual solid. However, there has been only limited work related to the effect of autohydrolysis pretreatment on the structural transformations occurring in the lignin fraction. The aim of this work was to characterize the changes in lignin structure during autohydrolysis of aspen wood. The residual lignin (MWL) in the hydrolyzed chips was systematically characterized by Fourier-transform infrared (FTIR),  $^1\text{H}$ , quantitative  $^{13}\text{C}$ ,  $^{31}\text{P}$ , and two-dimensional heteronuclear single quantum coherence (2D HSQC) nuclear magnetic resonance (NMR) spectroscopies, gel permeation chromatography/multi-angle laser light scattering (GPC-MALLS), and thermal analysis. It is believed that these investigations will deepen the understanding of the fundamental lignin chemistry during the autohydrolysis process and promote the subsequent utilization of lignocellulosic biomass.

## EXPERIMENTAL

### Materials

Aspen wood (a mixture of *Populus × euramericana* ‘Guariento’ and *Populus × euramericana* ‘Neva’) chips, which were approximately 2.0 to 3.5 cm long, 1.2 to 2.0 cm wide, and 0.5 cm thick, were kindly provided by Huatai Group Co. Ltd. (China). The clean chips obtained after washing and drying were kept in sealed bags and stored in a freezer at  $-25\text{ }^\circ\text{C}$ . Dioxane, 1,2-dichloroethane, alcohol, pyridine, and acetic anhydride were purchased from Sinopharm Chemical Reagent Co. Ltd. (China). Glacial acetic acid, petroleum ether, and toluene were procured from Tianjin Fuyu Chemical Reagent Co. Ltd. (China). Acetone and diethyl ether obtained from Laiyang Fine Chemical Factory (China).

### Methods

#### *Autohydrolysis*

The autohydrolysis, which used water as the only reagent, was carried out in a 15-L electrically heated and thermostatically controlled rotary digester (Xiyang Tongda Light Industrial Equipment Co. Ltd., China). The amount of aspen wood chips used for each experiment was approximately 1000 g (as oven-dried weight), and the solid-to-liquid ratio was set at 1:6. The autohydrolysis was operated at various final temperatures ( $T_{\text{max}}$ , ranging from 140 to 180  $^\circ\text{C}$ ). Approximately 25 min was needed to reach the desired  $T_{\text{max}}$ , and the isothermal treatment time was 60 min after reaching the  $T_{\text{max}}$ . When the autohydrolysis was finished, the mixture was rapidly cooled down to 75 to 77  $^\circ\text{C}$  within 20 min. After filtration, the solid fractions were thoroughly washed with water and oven-dried at 50  $^\circ\text{C}$  overnight for subsequent analysis.

### *Gross chemical analysis*

The untreated and autohydrolyzed aspen wood chips were analyzed for gross chemical composition, specified on an oven dry weight basis. The contents of holocellulose were determined according to China standard GB/T 2677.10 (1995). Pentosan content was determined according to standard GB/T 745 (2003). Klason lignin (acid-insoluble) and acid-soluble lignin were measured according to China standard GB/T 2677.8 (1994) and GB/T 10337 (2008). The amounts of benzene/ethanol extractable material were determined according to China standard GB/T 10741 (2008) using a Soxhlet extractor.

### *Isolation and purification of lignin*

Milled wood lignin (MWL) was isolated and purified from the untreated aspen wood chips as well as from the autohydrolyzed solid fractions, following the reported protocol (El Hage *et al.* 2009; Rencoret *et al.* 2009). The wood chips were milled using a Wiley mill to pass through a 0.5-mm screen mesh. Approximately 30 g of milled wood was treated with 600 mL ethanol/benzene mixture (1:2, v/v) for 24 h in a Soxhlet apparatus, followed by a 24-h Soxhlet extraction with 600 mL ethanol to remove extractives. Then, the milled wood was air dried, transferred to a stainless steel jar, and ground in a vibration ball mill (WL-1, China) for at least 72 h. Stainless steel balls of three different sizes and 200 mL of toluene were added to the milled wood prior to ball milling. After the extractive-free ball milled wood was dried to remove toluene, it was suspended in 96% aqueous dioxane (dioxane/water 96:4, v/v) with a solid-to liquid ratio of 1:25 (g:mL) and extracted twice in a shaker for 24 h in the dark. After centrifugation, the combined filtrates were concentrated with a rotary evaporator under reduced pressure to approximately 50 mL and were freeze-dried to obtain the rough milled wood lignin (MWL). Then, the rough MWL was dissolved in 90% acetic acid (20 mL) and precipitated in deionized water (500 mL) while stirring. After centrifugation, the precipitate was freeze-dried to obtain relatively pure MWL, which was subsequently dissolved in 1,2-dichloroethane/ethanol (10 mL, 2:1, v/v) and precipitated in diethyl ether (200 mL). The purified MWL obtained by centrifugation was washed with petroleum ether (2×100 mL), freeze-dried, and labeled as MWL<sub>0</sub>, MWL<sub>140</sub>, MWL<sub>170</sub>, and MWL<sub>180</sub>, respectively, according to the autohydrolysis temperatures (0, 140, 170, and 180 °C).

### *Fourier-transform infrared spectroscopy*

The FT-IR spectra of the lignin samples were obtained on a spectrophotometer (IR Prestige-21, Shimadzu, Japan) using the KBr pellet technique. Approximately 1 mg of lignin was mixed and thoroughly ground with approximately 100 mg of KBr to reduce particle size and to obtain uniform dispersion of the sample in the disks. Each spectrum was recorded over 10 scans, in the frequency range from 4000 to 500 cm<sup>-1</sup>, with a resolution of 0.5 cm<sup>-1</sup>. The fingerprint region was baseline corrected between 1900 and 750 cm<sup>-1</sup>.

### *NMR analysis*

The <sup>1</sup>H- and <sup>13</sup>C-NMR spectra of the lignin samples were recorded on a Bruker (Germany) AVIII 400-MHz spectrometer fitted with a 5-mm broadband probe with a gradient field in the Z-direction at room temperature in deuterated dimethyl sulfoxide (DMSO-d<sub>6</sub>) as the solvent. The lignin (60 mg) was placed into a 5-mm NMR tube and dissolved in 0.5 mL of DMSO-d<sub>6</sub> according to Wen *et al.* (2013b). The <sup>1</sup>H NMR spectrum was recorded on the spectrometer with a minimum of eight scans, a sweep width of 400

MHz, an acquisition time of 2.0 s, and a relaxation delay time of 3 s, while the  $^{13}\text{C}$  NMR spectrum was acquired with a minimum of 20,000 scans, a sweep width of 400 MHz, an acquisition time of 0.4 s, and a relaxation delay of 1.5 s.

For 2D HSQC spectra, a standard Bruker HSQC pulse sequence, “hsqcetgpsi2,” was used. Relative inter-unit linkage levels in lignins were estimated semi-quantitatively using volume integration of contours in 2D HSQC spectra, and the well-resolved  $\alpha$ -carbon contours were used for volume integration for  $\beta$ -O-4, resinol, and phenylcoumaran linkages (Pu *et al.* 2009).

$$\text{IC}_9 \text{ units} = 0.5 \text{ IS}_{2,6} + \text{IG}_2 \quad (1)$$

where  $\text{IS}_{2,6}$  is the integration of  $\text{S}_{2,6}$  including S and S', and  $\text{IG}_2$  is the integral value of  $\text{G}_2$ . The term  $\text{IC}_9$  represents the integral value of the aromatic ring (Sette *et al.* 2011; Wen *et al.* 2013b). According to the internal standard ( $\text{IC}_9$ ), the amount of  $\text{I}_x\%$  can be obtained using the following formula,

$$\text{I}_x (\%) = \text{I}_x / \text{IC}_9 \times 100 (\%) \quad (2)$$

where  $\text{I}_x$  is the integral value of the  $\alpha$ -position of A ( $\beta$ -O-4), B ( $\beta$ - $\beta$ ), and C ( $\beta$ -5), and the integration should be in the same contour level.

Quantitative  $^{31}\text{P}$  NMR spectra of the lignin samples were acquired according to published methods (Wen *et al.* 2013b; Guo *et al.* 2015). Approximately 40 mg of dried lignin was accurately weighed into a 5-mm NMR tube and dissolved in 650  $\mu\text{L}$  of anhydrous pyridine/ $\text{CDCl}_3$  (1.6:1, v/v), followed by injecting 50  $\mu\text{L}$  of an internal standard solution (N-hydroxy naphthalimide, 80 mg/mL, in anhydrous pyridine/ $\text{CDCl}_3$  (1.6:1, v/v)) and 50  $\mu\text{L}$  of a relaxation reagent (chromium (III) acetylacetonate, 11 mg/mL, in anhydrous pyridine/ $\text{CDCl}_3$  (1.6:1, v/v)). Then, 100  $\mu\text{L}$  of 2-chloro-4,4,5,5-tetramethyl-1,3,2-dioxaphospholane (TMDP) was added to the above solution and the mixture was maintained for 10 min. The final phosphorylated lignin was then subsequently analyzed employing an observation sweep width of 81,521.74 Hz. The acquisition time and relaxation delay parameter were 1.5 s and 2.0 s, respectively. A high signal/noise ratio of approximately 1000 transients was acquired during the NMR analysis.

#### GPC-MALLS analysis

The lignin samples were first acetylated with acetic anhydride. In brief, 60 mg of lignin was dissolved in 3 mL of pyridine/anhydride (1:2, v/v) and nitrogen gas was bubbled to drive the air out. Then, the reaction mixture was stirred for 72 h at room temperature in a dark environment. When the homogeneous reaction of lignin with acetic anhydride was finished, the solution was added dropwise to diethyl ether (40 mL), followed by centrifugation. The precipitate was washed three times with diethyl ether and dried under vacuum at 40  $^\circ\text{C}$  for 24 h. The weight-average molecular weights ( $M_w$ ) and polydispersity index (PDI) of the acetylated lignin dissolved in tetrahydrofuran (THF) were determined using a GPC-MALLS (DAWN HELEOS, Wyatt, USA) system. The sample concentration was 5 to 10 mg/mL and must be calculated to four decimal places. The laser light source was a 50-MW GaAs laser, and the wavelength of the laser was 658 nm.

#### Thermal analysis

Thermal degradation of the lignin samples was studied by thermogravimetric analysis (TGA), which was carried out on a thermal gravimetric analyzer (TGA Q50, TA

instruments, USA). Samples of ~5 mg that were vacuum dried at 40 °C for 48 h before measurement were heated from ambient temperature up to 600 °C at a rate of 10 °C/min, using a constant nitrogen flow as an inert atmosphere during the experiment.

Differential scanning calorimetry (DSC) analysis of the lignin samples was performed on a Mettler Toledo Instrument DSC823e (Switzerland) under a nitrogen atmosphere. Approximately 1.5 mg of the sample was first heated from -50 to 105 °C at a constant heating rate of 10 °C/min and then immediately cooled to -50 °C. Subsequently, the sample was again heated from -50 to 200 °C at 10 °C/min. The thermal behavior was analyzed based on the secondary heating traces.

## RESULTS AND DISCUSSION

### Effect of Autohydrolysis on the Gross Chemical Composition of Solid Fractions

The autohydrolysis pretreatments of aspen wood chips were carried out at maximum temperatures between 140 and 180 °C. Table 1 gives the yields and the chemical characterization results of the solid fractions obtained. The mass removal of the chips increased with pretreatment temperature. The yield of solid fractions after autohydrolysis at 170 °C for 60 min was approximately 83%, implying that approximately 17% of materials were dissolved and dispersed into process water during the autohydrolysis process. As expected, autohydrolysis primarily caused the hemicellulose polysaccharides (mostly xylans) to depolymerize. Approximately half of the original xylans could be removed from the chips and solubilized in the water effluent, whereas the amount of cellulose in the solid fractions showed that little cellulose degradation was caused by autohydrolysis treatment.

**Table 1.** Gross Chemical Compositions of Aspen Wood and Processed Solid Fractions after Autohydrolysis at Various Temperatures

	Yield (%)	Extractives <sup>a</sup> (%)	Pentosan <sup>a</sup> (%)	Cellulose <sup>a</sup> (%)	Lignin <sup>a</sup> (%)		
					Total	Klason	Acid soluble
Raw	100	3.05	19.39	46.59	23.43	20.86	2.57
140 °C	93.40	3.81	16.21	44.72	23.84	19.53	4.31
150 °C	89.56	4.66	14.93	44.55	21.93	17.48	4.45
160 °C	85.38	5.09	12.65	43.89	19.60	15.72	3.88
170 °C	83.14	6.14	10.18	42.03	17.19	13.55	3.64
180 °C	75.34	6.72	9.47	40.41	17.24	13.89	3.35

<sup>a</sup> The chemical compositions were based on un-pretreated aspen wood.

By comparison of the lignin content in the wood chips before and after the autohydrolysis treatment, it is assumed that only a limited proportion of lignin could be solubilized into the process water. Table 1 shows that almost no solubilization of lignin occurred under the autohydrolysis conditions of 140 °C and 60 min. After pretreating for 60 min at 170 °C, the Klason lignin content decreased to 13.55% (based on unpretreated aspen wood). It needs to be mentioned that the content of lignin in the solid fraction increased when the autohydrolysis temperature further increased up to 180 °C. This increase can be associated with the condensation reactions of lignin with reactive

hemicellulose degradation products, such as furfural, and the re-adsorption and re-deposition of the produced pseudo-lignin and the dissolved lignin.

### Effect of Autohydrolysis on the Structure of Lignin

To understand how the autohydrolytic conditions affected the structure of lignin, the milled wood lignin was isolated from the unpretreated ( $MWL_0$ ) and autohydrolyzed aspen wood chips ( $MWL_{140}$ ,  $MWL_{170}$ , and  $MWL_{180}$ ) and analyzed by FT-IR,  $^1H$  NMR,  $^{13}C$  NMR, 2D HSQC NMR,  $^{31}P$  NMR, GPC-MALLS, TGA, and DSC.

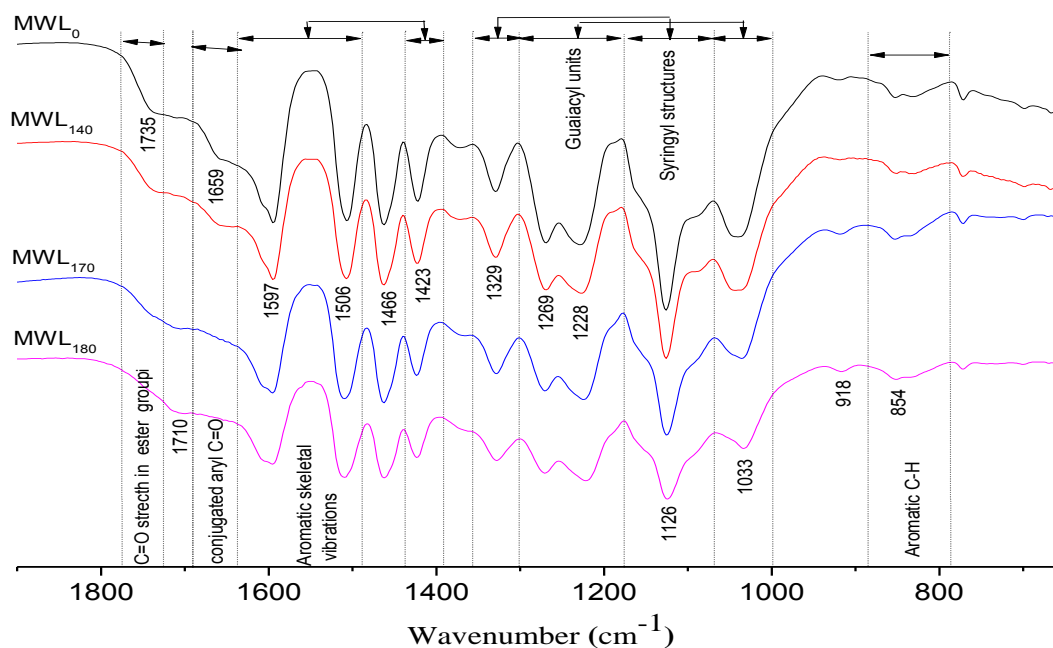


**Fig. 1.** FT-IR of  $MWL_0$ ,  $MWL_{140}$ ,  $MWL_{170}$ , and  $MWL_{180}$  corresponding to lignin isolated from native aspen wood and the autohydrolyzed solid residue (140, 170, and 180 °C)

#### FT-IR spectra of the lignin

The FT-IR spectra (fingerprint regions) obtained for the lignin samples are shown in Fig. 1. The vibration bands of typical functional groups associated with the lignin structure were found in the FT-IR spectra: carbonyl stretching in ester groups ( $1735\text{ cm}^{-1}$ ), conjugated/unconjugated carboxyl acid/ester groups or unconjugated  $\beta$ -ketone carbonyl groups ( $1710\text{ cm}^{-1}$ ) (Wang *et al.* 2012), conjugated aryl carbonyl stretching ( $1659\text{ cm}^{-1}$ ), aromatic skeleton vibrations ( $1597$ ,  $1506$ , and  $1423\text{ cm}^{-1}$ ), C-H deformations ( $1466\text{ cm}^{-1}$ ), aromatic C-H out of plane bending ( $854\text{ cm}^{-1}$ ), guaiacyl lignin units ( $1269$ ,  $1228$ , and  $1033\text{ cm}^{-1}$ ), and syringyl structures in lignin molecules ( $1329$  and  $1126\text{ cm}^{-1}$ ) (Sun *et al.* 2000; Xiao *et al.* 2012; Sun *et al.* 2015). The four lignin samples had rather similar FT-IR spectra, indicating that the residual lignin in the autohydrolyzed aspen wood chips had not undergone major structural modifications. However, the lignin samples obtained by autohydrolysis under various temperatures showed different intensities in some bands. The gradual disappearance of the relative intensities of ester structures at  $1735\text{ cm}^{-1}$  and of conjugated aryl carbonyl groups at  $1659\text{ cm}^{-1}$ , and the formation of unconjugated  $\beta$ -ketone carbonyl groups at  $1710\text{ cm}^{-1}$  with increasing autohydrolysis temperature, are clearly discernible (Li *et al.* 2008; Wang *et al.* 2012), which is due to the destruction of the  $\beta$ -O-4

linkages during autohydrolysis process. Additionally, the cleavage of the ether linkages in the corresponding lignins also could be revealed by a slight decrease in the intensities of the bands at  $1329\text{ cm}^{-1}$  (C-O vibration of S rings) and  $1269\text{ cm}^{-1}$  (shoulder peak, C-O of G rings) with increasing autohydrolysis temperature.

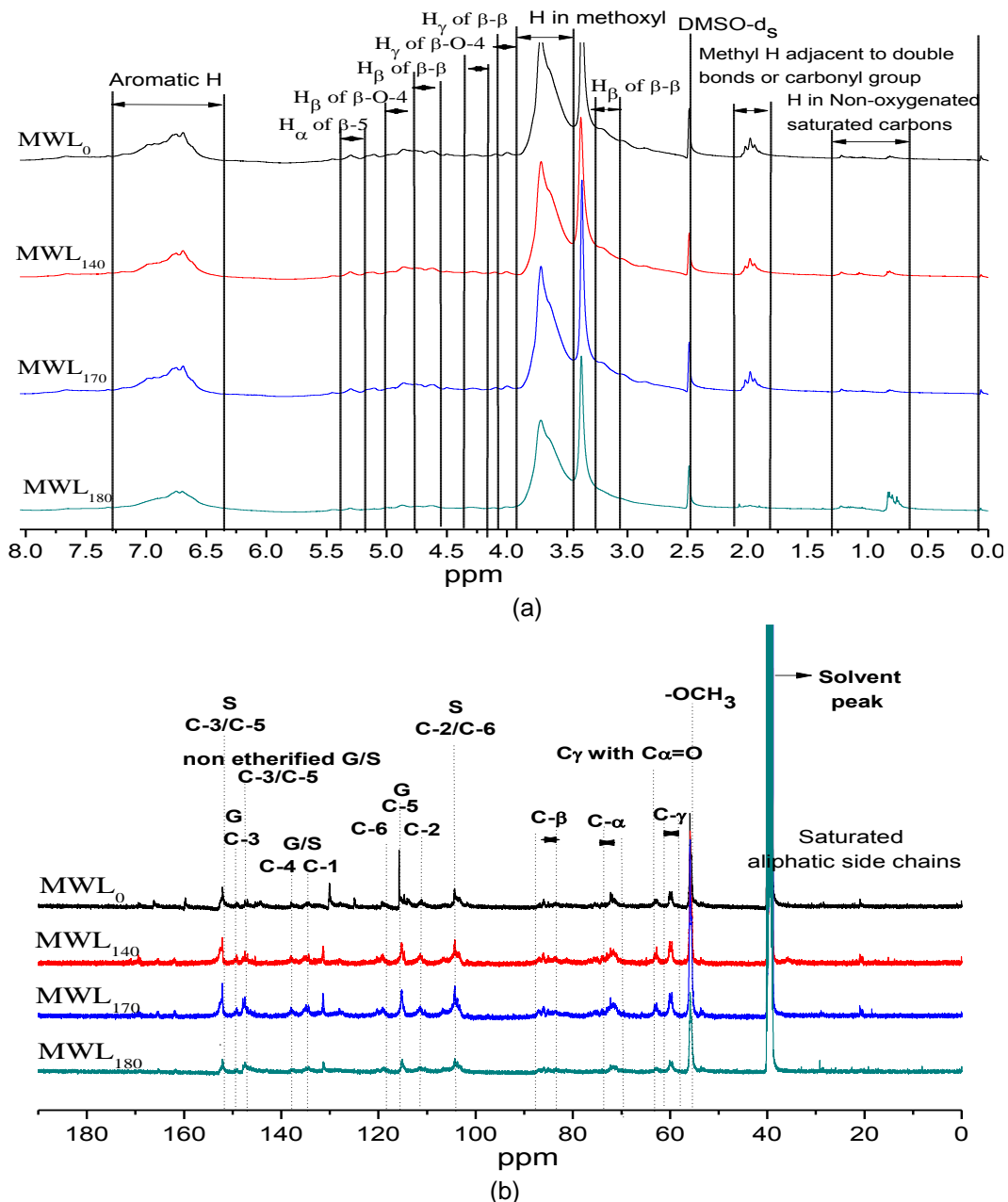


**Fig. 2.** (a)  $^1\text{H}$  NMR and (b)  $^{13}\text{C}$  NMR spectra of MWL<sub>0</sub>, MWL<sub>140</sub>, MWL<sub>170</sub>, and MWL<sub>180</sub>  $^1\text{H}$  and  $^{13}\text{C}$  NMR spectra of lignin

To further investigate the structural differences among the lignin samples, the  $^1\text{H}$  and  $^{13}\text{C}$  NMR spectra of the lignin samples were recorded; the corresponding peak assignments (Kim *et al.* 2011; Wang *et al.* 2012) are shown in Fig. 2. As can be seen from Fig. 2(a), the signals of aromatic protons of G- and S- units appeared at  $\delta$  6.6 to 7.2 ppm,

whereas the intensity of the signal corresponding to G units (at  $\delta$  7.0 to 7.2 ppm) gradually decreased and the intensity of the signal assigned to S units (at  $\delta$  6.6 to 6.7 ppm) gradually increased as the autohydrolysis temperature increased from 140 to 180 °C. Meanwhile, the intensity of signals at  $\delta$  4.1 to 4.8 ppm corresponding to the protons of the  $\beta$ -O-4 structure became much weaker with increasing autohydrolysis temperature, which is evidence for the cleavage of  $\beta$ -O-4 structures. In Fig. 2(b), the peaks of aromatic carbon in lignin units appeared at  $\delta$  151.9 ppm ( $C_{3,5}$  of etherified S-unit), 149.0 ppm ( $C_3$  of etherified G-unit), 147.4 ppm ( $C_{3,5}$  of non-etherified S- or G-units), 137.9 ppm ( $C_4$  of S- or G-units), 134.6 ppm ( $C_1$  of S- or G-units), 130.1 ppm ( $C_1$  of non-etherified S- or G-units), 118.1 ( $C_6$  of G-unit), 115.7 ppm ( $C_5$  of G-unit), 111.3 ppm ( $C_2$  of G-unit), and 104.5 ppm ( $C_{2,6}$  of S-unit). The peaks at  $\delta$  73.9 to 69.4, 87.5 to 83.5, and 61.0 to 58.6 ppm can be assigned to the  $C_\alpha$ ,  $C_\beta$ , and  $C_\gamma$  of  $\beta$ -O-4 linkages, respectively (Wen *et al.* 2013a). The signal at  $\delta$  62.7 ppm was assigned to  $C_\gamma$  with  $C_\alpha=O$  originating from side chain oxidation *via* hemolytic cleavage (Kim *et al.* 2011). The peaks of methoxyl carbon appeared at  $\delta$  55.4 ppm.

Table 2 shows the quantification of the methoxy groups and aromatic carbon in these lignin samples. The content of methoxy groups in MWL<sub>0</sub> was 76/100Ar, while it decreased to 67, 62, and 57 per 100Ar in MWL<sub>140</sub>, MWL<sub>170</sub>, and MWL<sub>180</sub>, respectively, indicating that some of methoxy groups were removed during autohydrolysis pretreatment. In addition, the degree of condensation of the residual lignin in autohydrolyzed aspen markedly increased with increasing autohydrolysis temperature, confirming that autohydrolysis pretreatment could cause the repolymerization of lignin units. As the condensation reactions that lead to repolymerization of the lignin may occur at electron-rich carbon atoms such as the C-2/C-6 present in guaiacyl and syringyl rings, the abundance of C-2 and C-6 groups of the G- and S- units indicated that the degree of condensation was much lower when it underwent autohydrolysis below 170 °C (Li and Gellerstedt 2008).

**Table 2.** Quantification of the Inter-Unit Linkages in the Lignin Samples by Quantitative <sup>13</sup>C NMR and 2D HSQC NMR

Lignin samples <sup>a</sup>	MWL <sub>0</sub>	MWL <sub>140</sub>	MWL <sub>170</sub>	MWL <sub>180</sub>
Methoxy groups <sup>b</sup>	76	67	62	57
H-Substituted aromatic C <sup>b</sup>	65	52	50	48
O-Substituted aromatic C <sup>b</sup>	25	25	24	19
C-Substituted aromatic C <sup>b</sup>	22	23	26	30
Degree of condensation <sup>c</sup>	0.72	0.82	1.00	1.02
$\beta$ -Aryl-ether units ( $\beta$ -O-4, A) <sup>d</sup>	64.3	62.5	51.1	40.2
Resinol substructures ( $\beta$ - $\beta$ , B) <sup>d</sup>	13.7	10.0	12.7	11.6
Phenylcoumaran ( $\beta$ -5, C) <sup>d</sup>	4.6	4.3	5.4	6.7

<sup>a</sup> Milled wood lignin.

<sup>b</sup> Quantification is based on the assumption that the aromatic region of the <sup>13</sup>C NMR spectra ( $\delta$  101.5 to 162 ppm) contains 600 aromatic carbon atoms; results expressed per 100 Ar.

<sup>c</sup> Degree of condensation = (C-substituted aromatic C + O-substituted aromatic C) / H-substituted aromatic C (Leschinsky *et al.* 2008b).

<sup>d</sup> Results expressed per 100 Ar based on quantitative 2D HSQC NMR.

### 2D HSQC NMR analysis

Detailed structural changes to the aspen lignin during autohydrolysis process were further characterized by 2D-HSQC NMR spectroscopy. Figure 3 shows the 2D-HSQC spectra and the identified structures of lignin samples (MWL<sub>0</sub>, MWL<sub>140</sub>, MWL<sub>170</sub>, and

MWL<sub>180</sub>). The aromatic region in the spectra of all lignin samples (Fig. 3, right) displays the basic lignin units S (syringyl units), S' (syringyl units with oxidized  $\alpha$ -ketone), G (guaiacyl units), and PB (*p*-hydroxybenzoate units), which are easily identified by their correlations at  $\delta_C/\delta_H$  104.0/6.7, 106.3/7.2, 111.0/7.0, 115.1/6.9, 119.2/6.8, and 131.3/7.7 ppm, corresponding to the S<sub>2,6</sub>, oxidized S<sub>2,6</sub>, G<sub>2</sub>, G<sub>5</sub>, G<sub>6</sub>, and PB<sub>2,6</sub> positions, respectively (Samuel *et al.* 2013). In the side-chain region, the inter-unit linkages and substructures such as methoxy groups,  $\beta$ -aryl ether ( $\beta$ -O-4, A), resinol ( $\beta$ - $\beta$ , B), phenylcoumaran ( $\beta$ -5, C), and spirodienone ( $\beta$ -1, D) can be observed at  $\delta_C/\delta_H$  55.6/3.7 (OMe), 71.9/4.9 (A <sub>$\alpha$</sub> ), 83.6/4.3 (A <sub>$\beta$</sub> ), 59.6/3.6 (A <sub>$\gamma$</sub> ), 84.8/4.7 (B <sub>$\alpha$</sub> ), 53.4/3.1 (B <sub>$\beta$</sub> ), 71.0/4.2 and 70.8/3.8 (B <sub>$\gamma$</sub> ), 87.2/5.5 (C <sub>$\alpha$</sub> ), 62.3/3.9 (C <sub>$\gamma$</sub> ) and 55.4/3.1 (D <sub>$\beta$</sub> ) ppm, respectively (Samuel *et al.* 2013).

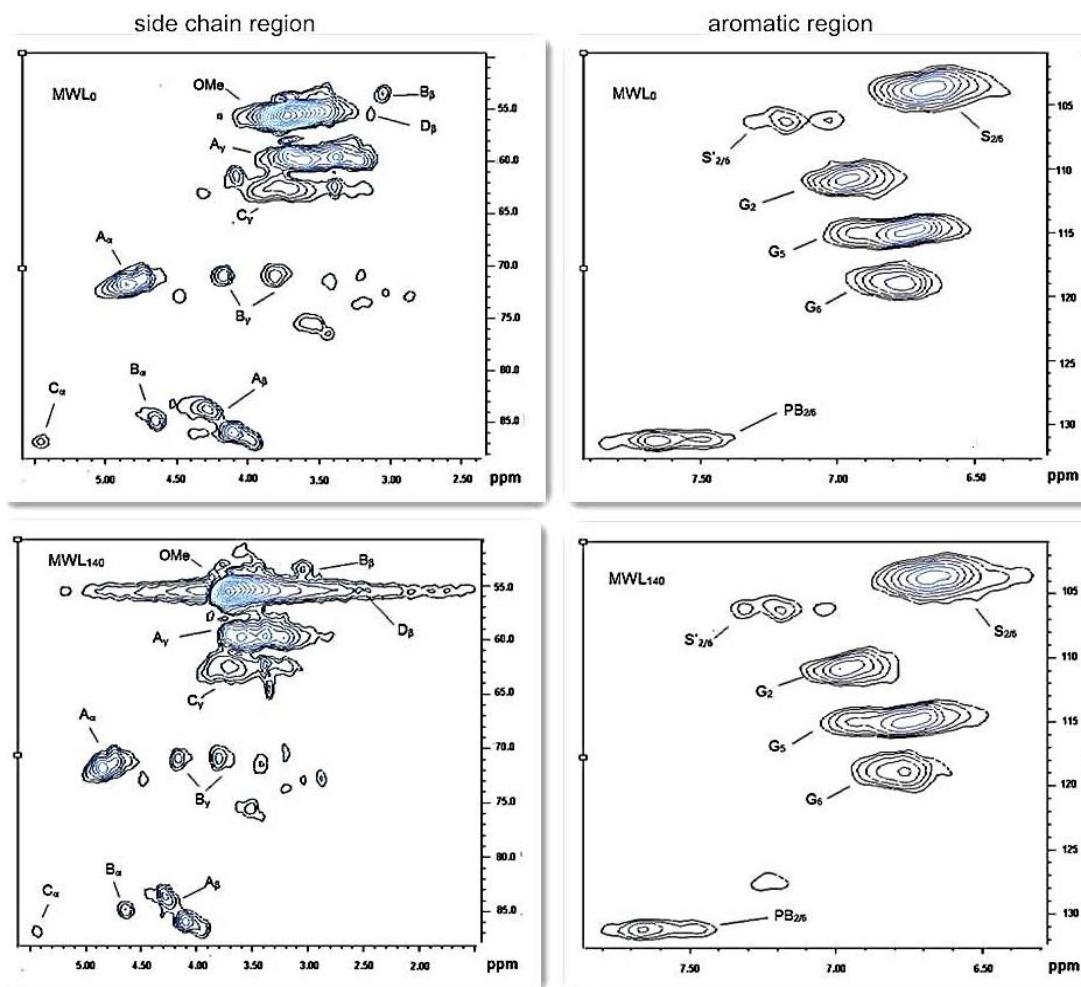


**Fig. 3 (first half).** 2D HSQC spectra of the lignin samples in DMSO-d<sub>6</sub> (left, the side-chain region and right, the aromatic region). Identified units include methoxy groups,  $\beta$ -O-4 ether (A), resinol ( $\beta$ - $\beta$ , B), phenylcoumaran ( $\beta$ -5, C), spirodienone ( $\beta$ -1, D), syringyl units (S), syringyl units with oxidized  $\alpha$ -ketone (S'), guaiacyl units (G), and *p*-hydroxybenzoate units (PB)

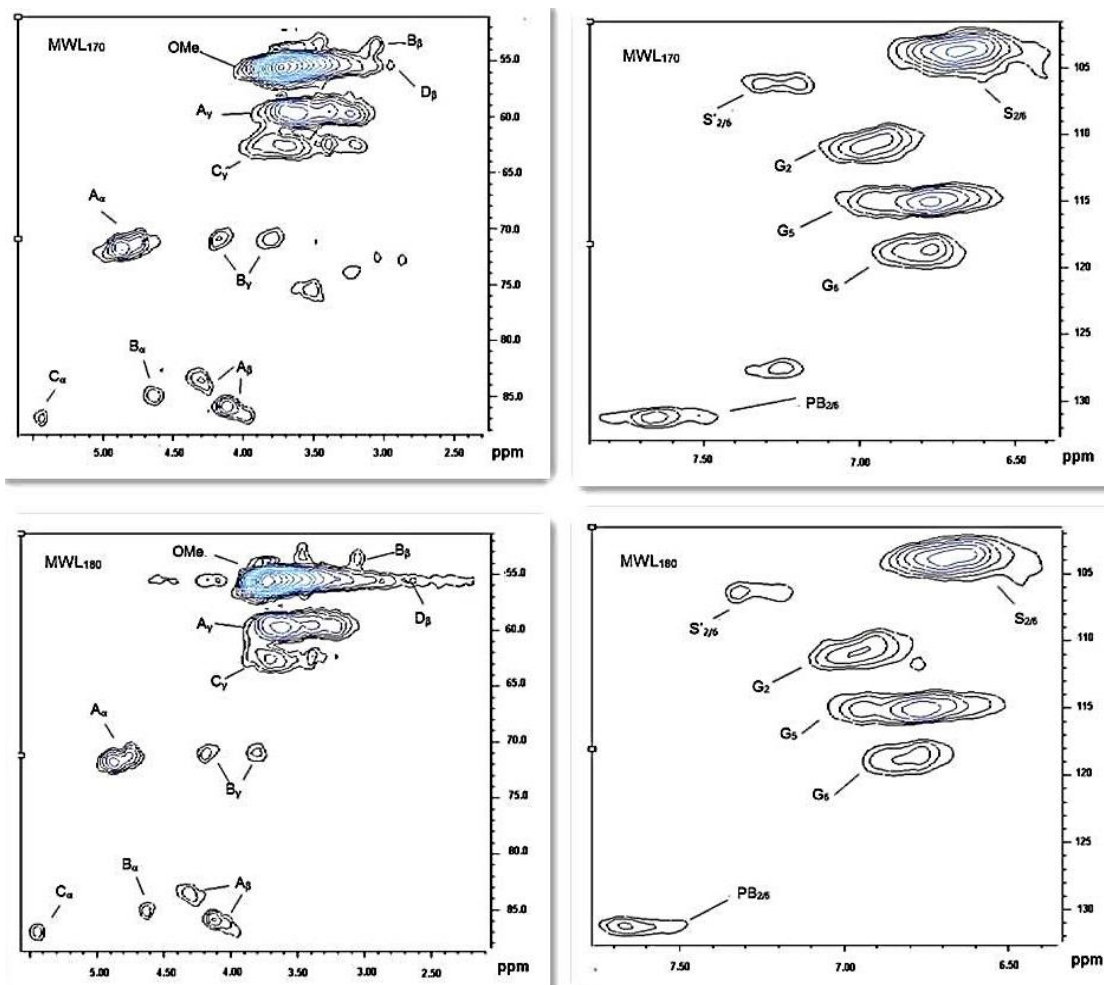


**Fig. 3 (second half).** 2D HSQC spectra of the lignin samples in DMSO-d<sub>6</sub> (left, the side-chain region and right, the aromatic region). Identified units include methoxy groups,  $\beta$ -O-4 ether (A), resinol ( $\beta$ - $\beta$ , B), phenylcoumararan ( $\beta$ -5, C), spirodienone ( $\beta$ -1, D), syringyl units (S), syringyl units with oxidized  $\alpha$ -ketone (S'), guaiacyl units (G), and *p*-hydroxybenzoate units (PB)

Quantification of the inter-unit linkages in these lignin samples is shown in Table 2. In the native aspen wood MWL<sub>0</sub>, the value of  $\beta$ -O-4 structures was 64.3/100Ar, which is rather close to the results of Li *et al.* (2007). The contents of  $\beta$ - $\beta$  and  $\beta$ -5 linkages in the MWL<sub>0</sub> were 13.7/100Ar and 4.6/100Ar, respectively. After autohydrolysis, the content of  $\beta$ -O-4 structures in MWL decreased successively with increasing autohydrolysis temperature.

Compared with native lignin, the  $\beta$ -O-4 content after autohydrolysis pretreatment at 140, 170, and 180 °C was reduced by 2.8%, 20.5%, and 37.5%, respectively. Moreover, the contents of  $\beta$ -5 linkages increased with increasing autohydrolysis temperature from 140 to 180 °C, further indicating that the condensation reaction between lignin units occurred during the autohydrolysis process.

#### *Changes to the hydroxyl groups in lignin*

For an in-depth elucidation of structural features of lignin molecules, the quantitative <sup>13</sup>P NMR technique was applied to explore the types and amount of hydroxyl groups in the lignin samples. The contents of aliphatic OH, phenolic OH, and carboxylic

OH are listed in Table 3. The majority of the hydroxyl groups in aspen lignin come from the aliphatic side-chain of lignin, which is consistent with the results of Samuel *et al.* (2013). After autohydrolysis pretreatment, a gradual reduction of the content of aliphatic OH accompanied by an obvious increase in phenolic OH with increasing autohydrolysis temperature was observed. The decrease in aliphatic OH content was probably due to the dehydration reactions through acid-catalyzed elimination reactions on the propyl side chains (El Hage *et al.* 2010), whereas the increase in syringyl and guaiacyl (S- and G-type) phenolic OH content with increasing autohydrolysis temperature was attributed to the extensive depolymerization of lignin through the cleavage of aryl ether linkages (Sun *et al.* 2015). The content of condensed phenolic OH increased with increasing autohydrolysis temperature, indicating that autohydrolysis also resulted in the condensation reactions of lignin to different extents with an increase in pretreatment severity. In addition, the rate of increase of the S-type phenolic OH was greater than that of the corresponding G-units. The ratio of S-type phenolic OH to G-type phenolic OH increased from 0.52 for MWL<sub>0</sub> to 0.66 for MWL<sub>140</sub>, 1.07 for MWL<sub>170</sub>, and 1.09 for MWL<sub>180</sub>. The increase in G-type phenolic OH may be attributed to either the cleavage of  $\beta$ -O-4 linkages or the demethylation reactions of the S-units (Rauhala *et al.* 2011). It can be concluded that the cleavage of the  $\beta$ -O-4 linkages of S-units is easier than that of G-units. Another possibility is that more G-units and *p*-hydroxyphenol units were involved in condensation reactions on the C-6 position because there was less steric hindrance.

**Table 3.** Hydroxyl Group Contents of MWL (mmol/g) Isolated from Unpretreated and Autohydrolyzed Aspen Wood Chips

Lignin samples	Aliphatic OH	Phenolic OH				Carboxylic acid
		Condensed	Non-condensed			
			Syringyl	Guaiacyl	<i>p</i> -Hydroxyl	
MWL <sub>0</sub>	4.66	0.15	0.23	0.44	0.28	0.12
MWL <sub>140</sub>	4.31	0.19	0.31	0.47	0.26	0.11
MWL <sub>170</sub>	3.78	0.41	0.62	0.58	0.22	0.12
MWL <sub>180</sub>	3.25	0.58	0.76	0.70	0.23	0.13

#### *Changes in the molecular weight of lignin*

Analysis by GPC-MALLS was implemented to determine the weight-average molecular weight ( $M_w$ ) and the polydispersity indices (PDIs) of the lignin samples to understand the variation of the polymerization degree of the lignin caused by autohydrolysis pretreatment. It can be seen from Table 4 that the aspen lignin has no marked change in molecular weight after undergoing autohydrolysis pretreatment at 140 °C for 60 min. However, when the autohydrolysis temperature increased to above 170 °C, the autohydrolysis pretreatment resulted in much higher molecular weight of lignin, compared to the  $M_w$  of MWL<sub>0</sub> ( $1.705 \times 10^4$  gmol<sup>-1</sup>), mostly because of the condensation reactions of lignin.

In addition, the PDI of the lignin gradually decreased with increasing autohydrolysis temperature. Although the autohydrolysis pretreatment could facilitate the cleavage of inter-unit bonds in lignin, producing smaller fragments of lignin with low molecular weight, the dissolution of these low-molecular weight lignin fragments and the condensation reaction of lignin worked together to promote the increase in molecular weight and the decrease in polydispersity. The results suggested that the autohydrolysis

pretreatment provided lignin with a relatively uniform fragment size and a higher number of condensed linkages.

**Table 4.** Weight-Average Molecular Weight ( $M_w$ ) and Polydispersity Index (PDI) of Lignin Samples Obtained from the Solid Fraction after the Autohydrolysis Process

Lignin samples	$M_w$ ( $\times 10^4$ g/mol)	$M_w/M_n$	$M_z/M_n$
MWL <sub>0</sub>	1.705	1.145	1.369
MWL <sub>140</sub>	1.861	1.136	1.404
MWL <sub>170</sub>	3.554	1.032	1.187
MWL <sub>180</sub>	4.810	1.021	1.065

### Influence of Autohydrolysis on the Thermal Properties of Lignin

The thermal properties of the lignin samples were studied by thermogravimetric analysis (TGA) and differential scanning calorimetry (DSC). The curves from TGA and DTG analysis of the lignin samples are shown in Fig. 4. The decomposition of lignin can be divided into three stages. The first stage of weight loss (below 120 °C) belongs to the evaporation of the residual water in the lignin samples (Wörmeyer *et al.* 2011). Heating from 200 to 400 °C results in the breakage of the inter-unit linkages of lignin and evaporation of monomeric phenols, causing the major weight loss stage. The weight loss stage above 400 °C can be attributed to the disintegration of the aromatic rings of lignin molecules (Wörmeyer *et al.* 2011).

The maximum decomposition rate ( $V_M$ ) of MWL<sub>140</sub> was the same as that of MWL<sub>0</sub> (0.42 %/°C), but the temperature ( $T_M$ ) corresponding to  $V_M$  shifted to a lower temperature region (291.1 °C) compared with the  $T_M$  (301.1 °C) of MWL<sub>0</sub>. The results suggest that the lignin in the solid fractions autohydrolyzed at 140 °C was slightly easier to degrade compared with the lignin from the untreated aspen wood chips. However, the maximum decomposition rates ( $V_M$ ) for MWL<sub>170</sub> and MWL<sub>180</sub> were 0.37 and 0.36 %/°C, respectively, much lower than that for MWL<sub>0</sub> and MWL<sub>140</sub>, and the temperature ( $T_M$ ) corresponding to  $V_M$  shifted to a higher temperature region (340.5 and 359.3 °C for MWL<sub>170</sub> and MWL<sub>180</sub>, respectively). In addition, the non-volatile residues of MWL<sub>170</sub> (33.29%) and MWL<sub>180</sub> (37.12%) at 600 °C were higher than that of MWL<sub>0</sub> (26.28%) and MWL<sub>140</sub> (29.45%). Because the thermal properties of lignin polymers are affected by the inherent structure, various functional groups, degree of branching, and molecular weight (Sun *et al.* 2000), this difference reflects an increasing degree of branching and condensation of the MWL<sub>170</sub> and MWL<sub>180</sub> (Wang *et al.* 2012) samples. On the other hand, more “char residue” might result because of the decreased OCH<sub>3</sub> content in the MWL<sub>170</sub> and MWL<sub>180</sub> samples.

It can be observed from Fig. 4(c) that the differential scanning calorimetric (DSC) curve of MWL<sub>0</sub> presents a transition at 160 °C, whereas the glass transition temperatures ( $T_g$ ) of MWL<sub>140</sub>, MWL<sub>170</sub>, and MWL<sub>180</sub> were observed at 163, 173, and 187 °C, respectively. The higher  $T_g$  value for lignin samples isolated from autohydrolyzed aspen wood chips was caused by the limited free volume of lignin molecules as a result of repolymerization reactions. This, together with the increase in decomposition temperature, revealed that the autohydrolysis pretreatment process has a marked effect on the thermal stability of the residual lignin and the thermal stability of the lignin increased with the autohydrolysis temperature.

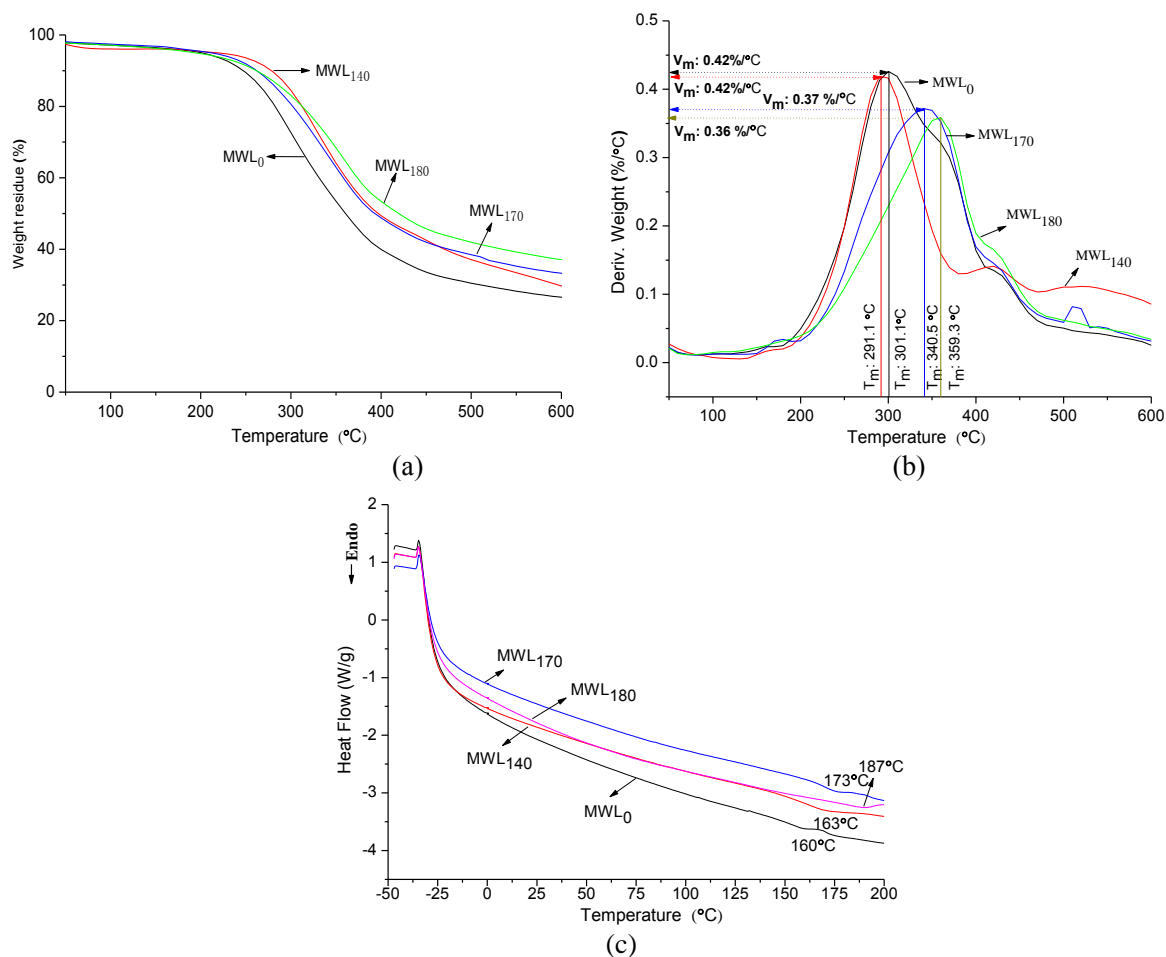


**Fig. 4.** (a) Thermogravimetric curves; (b) derivative thermogravimetric curves; and (c) DSC thermograms of MWL<sub>0</sub>, MWL<sub>140</sub>, MWL<sub>170</sub>, and MWL<sub>180</sub>

## CONCLUSIONS

1. Autohydrolysis pretreatment primarily caused the hemicellulose polysaccharides to depolymerize and be removed from the wood chips, whereas only a limited proportion of lignin and cellulose could be solubilized into the process water. However, the structure of the lignin remaining in the hydrolyzed chips was clearly changed during the autohydrolysis process.
2. The inter-unit linkages of  $\beta$ -O-4 were noticeable cleaved and the -OCH<sub>3</sub> groups were partly removed during the autohydrolysis pretreatment, leaving the residual lignin with more phenolic OH groups, fewer aliphatic OH groups, and higher syringyl OH /guaiacyl OH ratios.
3. However, the deconstruction of lignin was associated with the condensation reactions, which resulted in elevated amounts of C-C linkages and higher molecular weight of lignin. The repolymerization reaction seems to dominate when the autohydrolysis temperature is above 180 °C. To avoid the comprehensive condensation reactions of lignin, the autohydrolysis temperature should not exceed 170 °C at a given time of 60

min. Moreover, the autohydrolysis pretreatment could promote an increase in the thermal stability of lignin.

## ACKNOWLEDGEMENTS

The authors would like to acknowledge financial support from the National Natural Science Foundation of China (31540009 and 31370581), the Independent Innovation and Achievements Transformation Project of Shandong Province (2014CGZH0302), and the Yellow River Mouth Scholar Program (DYRC20120105).

## REFERENCES CITED

- Amidon, T. E., and Liu, S. J. (2009). "Water-based woody biorefinery," *Biotechnology Advances* 27(5), 542-550. DOI: 10.1016/j.biotechadv.2009.04.012
- Carvalho, F., Silva-Fernandes, T., Duarte, L. C., and Girão, F. M. (2009). "Wheat straw autohydrolysis: Process optimization and products characterization," *Applied Biochemistry and Biotechnology* 153(1), 84-93. DOI: 10.1007/s12010-008-8448-0
- Chen, X. W., Lawoko, M., and van Heiningen, A. (2010). "Kinetics and mechanism of autohydrolysis of hardwoods," *Bioresource Technology* 101(20), 7812-7819. DOI: 10.1016/j.biortech.2010.05.006
- El Hage, R., Brosse, N., Chrusciel, L., Sanchez, C., Sannigrahi, P., and Ragauskas, A. (2009). "Characterization of milled wood lignin and ethanol organosolv lignin from *miscanthus*," *Polymer Degradation and Stability* 94(10), 1632-1638. DOI: 10.1016/j.polymdegradstab.2009.07.007
- El Hage, R., Chrusciel, L., Desharnais, L., and Brosse, N. (2010). "Effect of autohydrolysis of *Miscanthus x giganteus* on lignin structure and organosolv delignification," *Bioresource Technology* 101(23), 9321-9329. DOI: 10.1016/j.biortech.2010.06.143
- Fasching, M., Griehl, A., Kandioller, G., Zieher, A., Weber, H., and Sixta, H. (2005). "Prehydrolysis sulfite revisited," *Macromolecular Symposia* 223(1), 225-238. DOI: 10.1002/masy.200550516
- GB/T 745 (2003). "Fibrous raw material – Determination of pentosan," Chinese National Standardization Management Committee, China.
- GB/T 2677.8 (1994). "Fibrous raw material – Determination of Klason lignin," Chinese National Standardization Management Committee, China.
- GB/T 2677.10 (1995). "Fibrous raw material – Determination of holocellulose," Chinese National Standardization Management Committee, China.
- GB/T 10337 (2008). "Fibrous raw material – Determination of acid soluble lignin," Chinese National Standardization Management Committee, China
- GB/T 10741 (2008). "Fibrous raw material – Determination of organic solvent extract," Chinese National Standardization Management Committee, China
- García, J. C., Zamudio, M. A. M., Pérez, A., López, F., and Colodette, J. L. (2011). "Search for optimum conditions of *Paulownia* autohydrolysis process and influence in pulping process," *Environmental Progress and Sustainable Energy* 30(1), 92-101. DOI: 10.1002/ep.10442

- Guo, Y. Z., Zhou, J. H., Wen, J. L., Sun, G. W., and Sun, Y. J. (2015). "Structural transformations of triploid of *Populus tomentosa* Carr. lignin during auto-catalyzed ethanol organosolv pretreatment," *Industrial Crops and Products* 76(15), 522-529. DOI: 10.1016/j.indcrop.2015.06.020
- Gütsch, J. S., Nousiainen, T., and Sixta, H. (2012). "Comparative evaluation of autohydrolysis and acid-catalyzed hydrolysis of *Eucalyptus globulus* wood," *Bioresource Technology* 109, 77-85. DOI: 10.1016/j.biortech.2012.01.018
- Hou, Q. X., Wang, Y., Liu, W., Liu, L. H., Xu, N. P., and Li, Y. (2014). "An application study of autohydrolysis pretreatment prior to poplar chemi-thermomechanical pulping," *Bioresource Technology* 169, 155-161. DOI: 10.1016/j.biortech.2014.06.091
- Jääskeläinen, A. S., Sun, Y., Argyropoulos, D. S., Tamminen, T., and Hortling, B. (2003). "The effect of isolation method on the chemical structure of residual lignin," *Wood Science and Technology* 37(2), 91-102. DOI: 10.1007/s00226-003-0163-y
- Kim, J. Y., Shin, E. J., Eom, I. Y., Won, K., Kim, Y. H., Choi, D., Choi, I. G., and Choi, J. W. (2011). "Structural features of lignin macromolecules extracted with ionic liquid from poplar wood," *Bioresource Technology* 102(19), 9020-9025. DOI: 10.1016/j.biortech.2011.07.081
- Leschinsky, M., Zuckerstätter, G., Weber, H. K., Patt, R., and Sixta, H. (2008a). "Effect of autohydrolysis of *Eucalyptus globulus* wood on lignin structure. Part 1: Comparison of different lignin fractions formed during water prehydrolysis," *Holzforschung* 62(6), 645-652. DOI: 10.1515/HF.2008.117
- Leschinsky, M., Zuckerstätter, G., Weber, H. K., Patt, R., and Sixta, H. (2008b). "Effect of autohydrolysis of *Eucalyptus globulus* wood on lignin structure. Part 2: Influence of autohydrolysis intensity," *Holzforschung* 62(6), 653-658. DOI: 10.1515/HF.2008.133
- Ligero, P., van der Kolk, J. C., de Vega, A., and van Dam, J. E. G. (2011). "Production of xylo-oligosaccharides from *Miscanthus × giganteus* by autohydrolysis," *BioResources* 6(4), 4417-4429. DOI: 10.15376/biores.6.4.4417-4429
- Li, J. B., and Gellerstedt, G. (2008). "Improved lignin properties and reactivity by modifications in the autohydrolysis process of aspen wood," *Industrial Crops and Products* 27(2), 175-181. DOI: 10.1016/j.indcrop.2007.07.022
- Li, S. M., Lundquist, K., and Westermarck, U. (2000). "Cleavage of arylglycerol  $\beta$ -aryl ethers under neutral and acid conditions," *Nordic Pulp and Paper Research Journal* 15(4), 292-299. DOI: 10.3183/NPPRJ-2000-15-04-p292-299
- Li, J. B., Henriksson, G., and Gellerstedt, G. (2007). "Lignin depolymerization/repolymerization and its critical role for delignification of aspen wood by steam explosion," *Bioresource Technology* 98(16), 3061-3068. DOI: 10.1016/j.biortech.2006.10.018
- Liu, S. J. (2010). "Woody biomass: Niche position as a source of sustainable renewable chemicals and energy and kinetics of hot-water extraction/hydrolysis," *Biotechnology Advances* 28(5), 563-582. DOI: 10.1016/j.biotechadv.2010.05.006
- Pu, Y. Q., Chen, F., Ziebell, A., Davison, B. H., and Ragauskas, A. J. (2009). "NMR characterization of C3H and HCT down-regulated alfalfa lignin," *BioEnergy Research* 2(4), 198-208. DOI: 10.1007/s12155-009-9056-8
- Rauhala, T., King, A. W. T., Zuckerstätter, G., Suuronen, S., and Sixta, H. (2011). "Effect of autohydrolysis on the lignin structure and the kinetics of delignification of birch

- wood,” *Nordic Pulp and Paper Research Journal* 26(4), 386-391
- Rencoret, J., Marques, G., Gutiérrez, A., Nieto, L., Jiménez-Barbero, J., Martínez, Á. T., and del Río, J. C. (2009). “Isolation and structural characterization of the milled-wood lignin from *Paulownia fortunei* wood,” *Industrial Crops and Products* 30(1), 137-143. DOI: 10.1016/j.indcrop.2009.03.004
- Ruiz, H. A., Rodríguez-Jasso, R. M., Fernandes, B. D., Vicente, A. A., and Teixeira, J. A. (2013). “Hydrothermal processing, as an alternative for upgrading agriculture residues and marine biomass according to the biorefinery concept: A review,” *Renewable and Sustainable Energy Reviews* 21, 35-51. DOI: 10.1016/j.rser.2012.11.069
- Samuel, R., Cao, S. L., Das, B. K., Hu, F., Pu, Q., and Ragauskas, A. J. (2013). “Investigation of the fate of poplar lignin during autohydrolysis pretreatment to understand the biomass recalcitrance,” *RSC Advances* 3(16), 5305-5309. DOI: 10.1039/C3RA40578H
- Sette, M., Wechselberger, R., and Crestini, C. (2011). “Elucidation of lignin structure by quantitative 2D NMR,” *Chemistry - A European Journal* 17(34), 9529-9535. DOI: 10.1002/chem.201003045
- Sun, R. C., Tomkinson, J., and Jones, G. L. (2000). “Fractional characterization of ash-AQ lignin by successive extraction with organic solvents from oil palm EFB fibre,” *Polymer Degradation and Stability* 68(1), 111-119. DOI: 10.1016/S0141-3910(99)00174-3
- Sun, S. N., Li, H. Y., Cao, X. F., Xu, F., and Sun, R. C. (2015). “Structural variation of eucalyptus lignin in a combination of hydrothermal and alkali treatments,” *Bioresource Technology* 176, 296-299. DOI: 10.1016/j.biortech.2014.11.030
- van Heiningen, A. (2006). “Converting a kraft pulp mill into an integrated forest biorefinery,” *Pulp and Paper-Canada* 107(6), 38-43.
- Wang, K., Jiang, J. X., Xu, F., and Sun, R. C. (2012). “Effects of incubation time on the fractionation and characterization of lignin during steam explosion pretreatment,” *Industrial and Engineering Chemistry Research* 51(6), 2704-2713. DOI: 10.1021/ie2016009
- Wen, J. L., Sun, S. L., Xue, B. L., and Sun, R. C. (2013a). “Quantitative structures and thermal properties of birch lignins after ionic liquid pretreatment,” *Journal of Agricultural and Food Chemistry* 61(3), 635-645. DOI: 10.1021/jf3051939
- Wen, J. L., Sun, S. L., Xue, B. L., and Sun, R. C. (2013b). “Recent advances in characterization of lignin polymer by solution-state nuclear magnetic resonance (NMR) methodology,” *Materials* 6(1), 359-391. DOI: 10.3390/ma6010359
- Wen, J. L., Sun, S. N., Yuan, T. Q., Xu, F., and Sun, R. C. (2013c). “Fractionation of bamboo culms by autohydrolysis, organosolv delignification and extended delignification: Understanding the fundamental chemistry of the lignin during the integrated process,” *Bioresource Technology* 150, 278-286. DOI: 10.1016/j.biortech.2013.10.015
- Wörmeyer, K., Ingram, T., Saake, B., Brunner, G., and Smirnova, I. (2011). “Comparison of different pretreatment methods for lignocellulosic materials. Part II: Influence of pretreatment on the properties of rye straw lignin,” *Bioresource Technology* 102(5), 4157-4164. DOI: 10.1016/j.biortech.2010.11.063
- Xiao, L. P., Shi, Z. J., Xu, F., and Sun, R. C. (2012). “Characterization of MWLs from *Tamarix ramosissima* isolated before and after hydrothermal treatment by

- spectroscopical and wet chemical methods,” *Holzforschung* 66(3), 295-302. DOI: 10.1515/HF.2011.154
- Xiao, L. P., Shi, Z. J., Xu, F., and Sun, R. C. (2013). “Characterization of lignins isolated with alkaline ethanol from the hydrothermal pretreated *Tamarix ramosissima*,” *BioEnergy Research* 6(2), 519-532. DOI: 10.1007/s12155-012-9266-3
- Zakaria, M. R., Hirata, S., and Hassan, M. A. (2015). “Hydrothermal pretreatment enhanced enzymatic hydrolysis and glucose production from oil palm biomass,” *Bioresource Technology* 176, 142-148. DOI: 10.1016/j.biortech.2014.11.027
- Zamudio, M. A. M., Alfaro, A., de Alva, H. E., García, J. C., García-Morales, M., and López, F. (2015). “Biorefinery of paulownia by autohydrolysis and soda-anthraquinone delignification process. Characterization and application of lignin,” *Journal of Chemical Technology and Biotechnology* 90(3), 534-542. DOI: 10.1002/jctb.4345
- Zhu, J. Y., and Pan, X. J. (2010). “Woody biomass pretreatment for cellulosic ethanol production: Technology and energy consumption evaluation,” *Bioresource Technology* 101(13), 4992-5002. DOI: 10.1016/j.biortech.2009.11.007
- Zhu, M. Q., Wen, J. L., Su, Y. Q., Wei, Q., and Sun, R. C. (2015). “Effect of structural changes of lignin during the autohydrolysis and organosolv pretreatment on *Eucommia ulmoides* Oliver for an effective enzymatic hydrolysis,” *Bioresource Technology* 185, 378-385. DOI: 10.1016/j.biortech.2015.02.061

Article submitted: January 5, 2016; Peer review completed: February 2, 2016; Revised version received and accepted: March 2, 2016; Published: March 18, 2016.  
DOI: 10.15376/biores.11.2.4086-4103